Detection of glaucoma using Neuroretinal Rim information

Conference Paper · December 2016

DOI: 10.1109/ICADW.2016.7942538

CITATIONS
7

READS
871

3 authors:

Pranjal Das
Gauhati University
2 PUBLICATIONS **19** CITATIONS
SEE PROFILE

S. R. Nirmala
Gauhati University
46 PUBLICATIONS **289** CITATIONS
SEE PROFILE

Jyoti Prakash Medhi
IIT Guwahati and Gauhati University
12 PUBLICATIONS **116** CITATIONS
SEE PROFILE

Detection of Glaucoma Using Neuroretinal Rim Information

Pranjal Das
Department of ECE,
Gauhati University,
Assam, India
Email: pranjald255@gmail.com

S. R. Nirmala
Department of ECE,
Gauhati University,
Assam, India
Email: nirmalasr3@gmail.com

Jyoti Prakash Medhi
Department of ECE,
Gauhati University,
Assam, India
Email: jpmedhi1@gmail.com

***Abstract*—Glaucoma is one of the most common causes of blindness in the world. The vision lost due to glaucoma cannot be regained. Early detection of glaucoma is thus very important. The Optic Disk(OD), Optic Cup(OC) and Neuroretinal Rim(NRR) are among the important features of a retinal image that can be used in the detection of glaucoma. In this paper, a computer-assisted method for the detection of glaucoma based on the ISNT rule is presented. The OD and OC are segmented using watershed transformation. The NRR area in the ISNT quadrants is obtained from the segmented OD and OC. The method is applied on the publicly available databases HRF, Messidor, DRIONS-DB, RIM-ONE and a local hospital database consisting of both normal and glaucomatous images. The proposed method is simple, computationally efficient and achieves a sensitivity of 91.82% and an overall accuracy of 94.14%.**

Keywords*—glaucoma, ISNT rule, Neuroretinal Rim, retinal image.

I. Introduction

Glaucoma is a disease of the eye causing optic nerve damage. It is the second leading cause of blindness in the world [1], [2]. The patients suffering from glaucoma are quite unaware of the disease until it has reached an acute stage, hence the name "the silent thief of sight". The progression of the disease occurs over a long interval of time resulting in slow but gradual loss of vision. Although the disease is incurable, however if detected in proper time its progression can be stopped.

Figure 1 illustrates the three important features of a retinal image- Optic Disk (OD), Optic Cup (OC) and Neuroretinal Rim (NRR). The OD acts as the entry and exit point for the central retinal artery and veins. The color of a normal OD is usually orange-pink but appears pale in presence of pathologies. OC is the central cavity in the OD. It is a cup-like structure and is devoid of nerve fibres [3]. The neuroretinal rim forms the outer boundary of the OC and lies between the edge of the OD and the OC. The NRR is that region of the OD that occupies the retinal nerve fibre axons. The presence of pathologies in the OD changes the shape of the NRR.

The intraocular fluid present in the eye exerts pressure on the eye known as the intraocular pressure (IOP). The IOP increases when the drainage system of the eye gets occluded. This rise in IOP, results in the damage of the optic nerve fibers.

978-1-5090-4291-3/16/$31.00

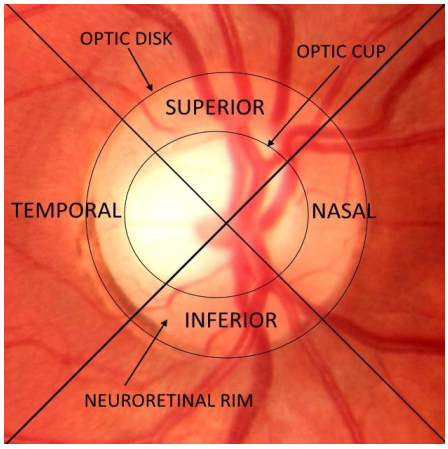

Fig. 1. Retinal image showing the OD, OC, NRR and the ISNT quadrants.

As the intensity of the damage increases, the OD begins to get depressed and develops a cupped shape [4]. There is a gradual expansion of the OC as the disease advances which results in progressive visual loss [5]. This increase in cup area is examined by evaluating the Cup-to-Disk Ratio (CDR). Clinically, the CDR is defined as the ratio of the vertical cup diameter to the vertical disk diameter. The CDR value is small for normal OD, while it is large for glaucomatous disks.

The Neuroretinal rim can be partitioned into four quadrants: Inferior (I), Superior(S), Nasal (N) and Temporal (T) as shown in figure 1. In an healthy eye, the inferior (I) rim is usually thicker than the superior (S) rim, which is thicker than the nasal (N) rim, and the temporal (T) rim is the thinnest. This is known as the ISNT rule [5], [6]. For assessment of glaucoma using the ISNT rule, the NRR area in each of the quadrants has to evaluated. Accurate evaluation of the NRR area depends upon the accuracy in segmenting the OD and OC.

II. Literature Survey

Numerous methods have been reported in the literature for the screening of glaucoma. Various methods are available in literature regarding OD detection [7], [8], [9]. Aquino et al. [7] proposed a method involving morphological and edge detection techniques followed by Circular Hough Transform to obtain a circular OD boundary approximation. The OD boundary was extracted in both red and green plane from the RGB sub-image, and the better of the two segmentation results

was finally selected. The OD boundary was approximated by a circle using the Circular Hough Transform. The method was able to find the OD correctly in 1186 out of the 1200 images from the Messidor database yielding a success rate of 99%. An OD segmentation method based on region growing and morphological operations is proposed in Priyadharshini et al. [10]. Morphological operations are used to remove the blood vessels and later median filtering is used to smooth the resultant image. The OD is segmented using region growing algorithm. The method is simple and involves less computational complexity, but fails to detect the OD over a diverse range of images. Morales et al. [8] proposed a method for OD segmentation using Principal Component Analysis (PCA) and stochastic watershed transformation. PCA is used in the preprocessing stage to enhance the input images. The stochastic watershed transformation was applied on this image to obtain the OD. The method was evaluated on images from the DRIONS database and achieved an accuracy of 99.01%. The method shows an improvement for OD segmentation over other classical watershed segmentation methods. However, the method involves more computational complexity than other classical watershed segmentation methods.

There are a very few methods in literature regarding OC segmentation as compared to OD segmentation. Wyawahare et al. [11] proposed a novel method for OC segmentation using thresholding and canny edge detection method. Three thresholds for the R, G and B plane images was obtained by finding the maximum intensity values in the individual planes respectively. The approximated cup region was found based on the thresholds. Canny edge detection method was used to obtain the OC boundary, which was later approximated by a circle. The method achieved an accuracy of 96.5% evaluated on 370 images from the MESSIDOR database. An OC segmentation method based on radial gradient is proposed by Ingle and Mishra [12]. CLAHE was applied on the individual R, G and B plane images to enhance the input images. The 'G' plane from the resulting RGB color image was extracted and radial gradient was applied on this image. The approximate cup region was found from the gradient magnitude image and then component labeling was used to get the OC boundary. The main drawback of the proposed method is that the computational complexity is more as compared to the linear gradient based methods.

Narasimhan and Vijayarekha [1] used CDR and the ISNT ratio as the two main features for glaucoma evaluation. K-means clustering technique was used to extract the OD and OC, which were finally, approximated using an elliptical approximation. The CDR was evaluated as the ratio between the area of the OC to the area of the OD. The ISNT ratio was calculated by measuring the area of the blood vessels in ISNT quadrant. The performance of the method was analyzed on three different classifiers KNN, SVM and Bayes classifier. The method achieved a maximum classification rate of 95% for glaucoma detection for the SVM classifier. Kavitha et al. [13] proposed a method for glaucoma evaluation using the CDR and the ISNT rule for glaucoma evaluation. Component labeling was used to obtain the OD boundary. The OC was detected from the green plane using component analysis method and the boundary was obtained through active contour. The method uses different features like CDR, asymmetry between left and right eye, NRR area and ISNT rule to diagnose glaucoma. The method was tested on image datasets from a local hospital and shows promising results for glaucoma detection.

A brief review of various literatures reveals that the CDR and ISNT rule are the two most widely features for glaucoma evaluation. The proposed method uses the ISNT rule for the detection of glaucoma. It is seen that large OD have large cups, and so the CDR value in such cases may give erroneous results [13], [14]. The basic intuition behind the proposed method is that the ISNT rule provides better classification accuracy as compared to CDR as it is independent of the OD size [15]. The method has been implemented on a diverse range of images, including four publicly available databases and a local hospital database. Section III represents the proposed method. Results and discussion are shown in Section IV.

III. Proposed Method

The proposed method detects an input retinal image as normal or glaucomatous. The proposed method requires human intervention to obtain the region of interest (ROI). The ROI, which mainly consists of the OD region is obtained by manually cropping the input retinal images. The rest of the method is fully automatic. The various stages involved in the proposed method is shown in figure 2.

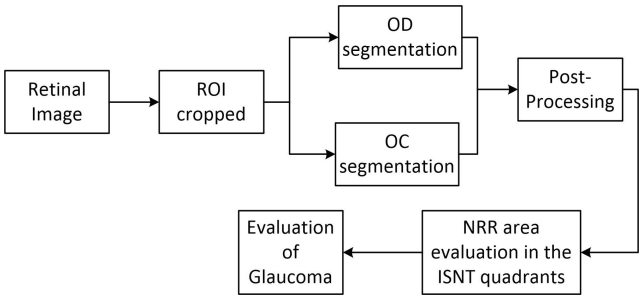

Fig. 2. Block Diagram of proposed method

The proposed method mainly consists of four stages -

1) OD segmentation: The OD is segmented from the cropped retinal images using watershed transformation. The 'R' plane of the RGB color space is taken for the segmentation purpose. The OD segmentation process is discussed in section III-A.
2) OC segmentation: The input retinal images which are manually cropped are converted to the Lab color space. Watershed transformation is applied on the 'a' plane to obtain the segmented OC. The OC segmentation process is discussed in section III-B.
3) Post processing: The segmented OD and OC are later approximated using a circular approximation. The procedure is discussed in section III-C.
4) Evaluation of Glaucoma: The NRR area is evaluated from the segmented OD and OC area by excluding the common region of the OD and OC from the OD area. The NRR area in different quadrants is evaluated by using different masks. The ISNT rule is used to classify an image as normal or glaucomatous. The evaluation procedure is discussed in section III-D.

A. OPTIC DISK SEGMENTATION

The OD appears to be uniform in the red channel of the RGB color space as can be seen from figure 3(b). Median

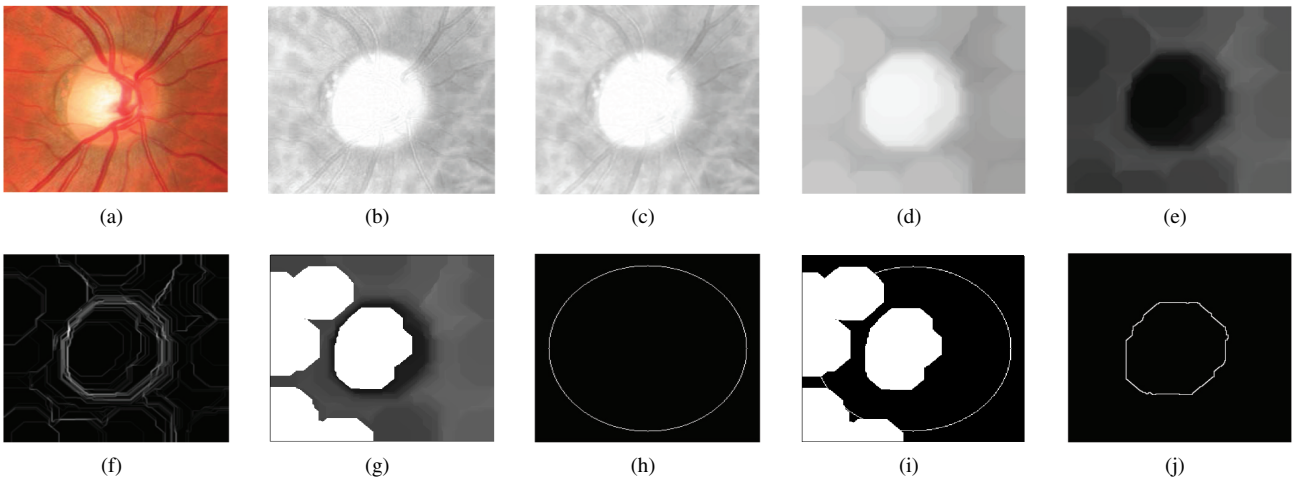

Fig. 3. (a) Original Cropped Fundus image, (b) Red plane image, (c) Median filtered image, (d) Opening, (e) Complemented image, (f) Gradient magnitude image, (g) Internal markers, (h) External marker, (i) Regional minima of the modified gradient magnitude image, (j) Segmented OD.

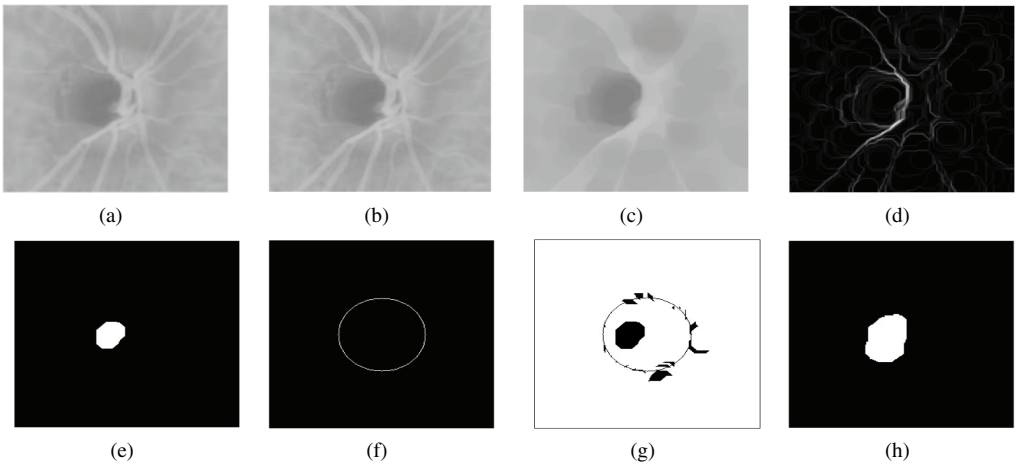

Fig. 4. (a) 'a'–plane image, (b) Median filtered image, (c) Closing, (d) Gradient Magnitude image, (e) Internal Marker, (f) External Marker, (g) Modified gradient magnitude image, (h) Segmented OC obtained by Watershed Transform.

filtering is applied on the extracted R plane image to remove the shading effect which occurs due to the presence of low frequency noise contents [16]. Figure 3(c) shows the median-filtered image. The obstructing blood vessels are removed by using grayscale morphological opening operation. The Structuring Element(SE) is chosen such that only the blood vessels are removed and the OD region is not affected. The size of SE determines the amount of blood vessels removed. In the proposed method, a disk shaped SE was used. Figure 3(d) shows the processed image after elimination of blood vessels. The watershed transformation interprets the regional minima in an image as the regions to be segmented. The OD region is transformed into a regional minimum by complementing the image obtained after the removal of blood vessels (figure 3(d)). The image is preprocessed prior to segmentation by obtaining the gradient magnitude of the image. The watershed transformation cannot be directly applied on the gradient magnitude image as it may produce oversegmentation due to the large number of regional minimum present in the image. The gradient-magnitude image is evaluated using the sobel operator. The gradient magnitude image is shown in figure 3(f). The gradient magnitude image is modified with the help of markers. The internal markers correspond to OD region and are evaluated by finding the regional minima in the complemented image (figure 3(e)). The external marker is given as a circle of constant diameter centered on the centroid of the image. The OD constitutes about 50% area in the cropped fundus image. Thus, the size of the circle is considered to be greater than 50% of the image-size. The external marker is shown in figure 3(h). The internal and external markers are used to modify the gradient magnitude image, so that regional minima occur only at the marked locations as can be seen in figure 3(i). The watershed transform is applied on the modified gradient image to get the segmented output as shown in figure 3(j).

B. OPTIC CUP SEGMENTATION

The segmentation of OC is considerably more challenging than OD segmentation due to the large portion of blood vessels circumscribing the OD. The cup region appears continuous and distinctive in the 'a' plane of the Lab color space as can be seen from figure 4(a).

Median filtering is performed on the 'a' plane image to eliminate the shading effect. The filtered image is shown in figure 4(b). The interfering blood vessels are removed

using morphological closing operation. A disk shaped structure element was used to eliminate the blood vessels. The image obtained after elimination of blood vessels is shown in figure 4(c). Marker-controlled watershed segmentation is used for OC segmentation. The gradient magnitude image as shown in figure 4(d) is obtained by applying the sobel operator on the blood vessels removed image of figure 4(c). The internal and external markers are used to modify the gradient magnitude image. The internal markers are evaluated by finding the regional minima in figure 4(c). The external marker is given as a circle of constant diameter centered on the centroid of the image. The size of the circle is approximated by about 25% of the image-size. The internal and external markers are shown in figure 4(e) and 4(f) respectively. Using minima imposition the gradient image is modified to have the regional minima only at the marked locations as shown in figure 4(g). The watershed segmentation algorithm is applied on this modified gradient image to get the segmented OC as shown in figure 4(h).

C. POST PROCESSING

The segmented OD and OC are superimposed on the RGB image as shown in figure 5(a). The segmented OD and OC are approximated using circular approximation and are shown in figure 5(b).

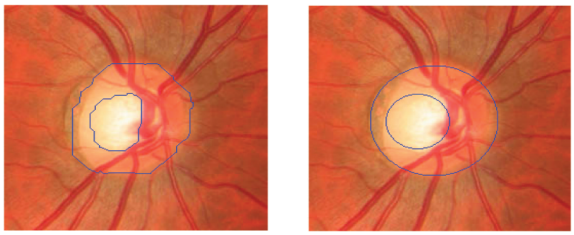

(a) (b)

Fig. 5. (a) Segmented OD and OC using watershed transformation, (b) Circular approximation of the final results.

D. EVALUATION OF GLAUCOMA

The NRR area is used in the detection of glaucoma. The NRR area in the different quadrants for a normal OD lies in the order:

$$Inferior \geq Superior \geq Nasal \geq Temporal$$

In glaucoma, the superior and inferior nerve fibres are damaged earlier than the temporal and nasal fibres. This causes the shrinking of the superior and inferior rims and thus violaton of the ISNT rule [6], [13].
The NRR region as shown in figure 6(a) is extracted by performing XOR operations on binary images of the segmented OD and OC. The NRR area in the ISNT quadrants can be calculated by applying different mask to the extracted NRR region. Figure 6(b)–6(e) shows the different masks used for extracting the NRR area in the ISNT quadrants. The results obtained are shown in figure 6(f)–6(i).

IV. RESULTS AND DISCUSSIONS

The assessment of the proposed method has been carried out on four publicly available databases: HRF [17], MESSIDOR [18], DRIONS-DB [19] and DIARETDB1 [20]. The images from a local eye hospital (Sri Sankaradeva Netralaya) are also used for evaluation of the proposed method.

The images obtained from the various sources are classified as normal or glaucomatous based on the ISNT rule. An image is classified as normal if it satisfies the ISNT rule and it is classified as glaucomatous if the ISNT rule is violated. The classification performance of the proposed method is assessed using the Sensitivity, Specificity and Accuracy measures.

TABLE I. RESULTS FOR DETECTION OF GLAUCOMA IMAGES

Image Sources	No. of Glaucomatous images	Correctly detected as glaucomatous	Sensitivity (%)
HRF	15	13	86.67
Messidor	29	27	93.10
DRIONS-DB	25	23	92
RIM-ONE	35	33	94.28
Local hospital	6	5	83.33
Total	110	101	91.82

Table I shows the sensitivity of the proposed method for different databases used. The proposed method correctly detects 101 retinal images as glaucomatous out of 110 glaucomatous retinal images with an overall sensitivity of 91.82%. From 182 normal images, 174 were correctly classified as normal with an overall specificity of 95.60%. The accuracy of the proposed method was found to be 94.14%. Table II shows the comparison of the proposed method with other methods available in the literature in terms of sensitivity, specificity and accuracy. The proposed method has been evaluated on a diverse range of images from different publicly databases and a local hospital database. The performance of proposed method in terms of sensitivity, specificity and accuracy is better as compared to the other methods.

Table III shows the comparison of the proposed method with three other methods which have been implemented on the same dataset. As observed from results shown in table III, the combined performance of proposed method in terms of sensitivity, specificity and accuracy is better as compared to the other three methods.

The proposed method failed in classifying some of the images due to poor illumination and presence of other pathologies in the OD region. The method produces some false-positives and false-negatives. Figure 7(a) shows an example of false-positives where a normal image is classified as glaucomatous by the proposed method. Figure 7(b) shows an example of false-negatives where a glaucomatous image is classified as normal by the proposed method.

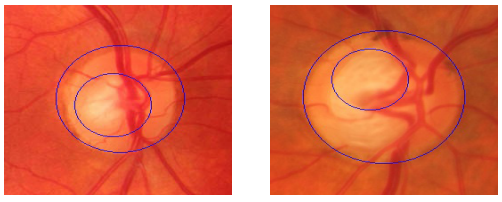

(a) (b)

Fig. 7. Example of: (a) false-positive and (b) false-negative.

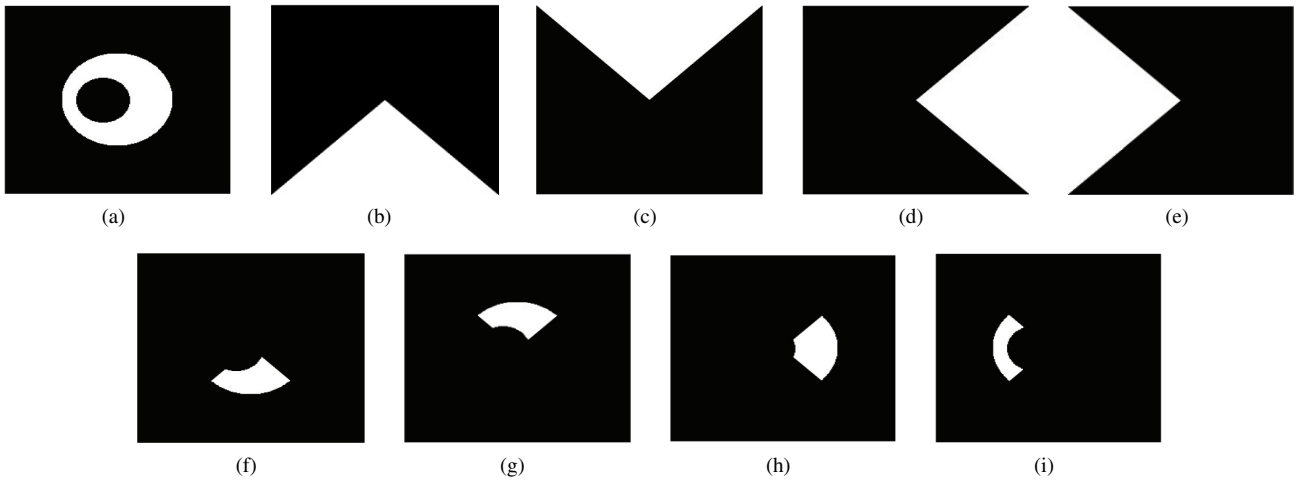

Fig. 6. (a) NRR area obtained from the segmented OD & OC, (b)–(e) : Mask for evaluation the NRR area in Superior, Inferior, Nasal and Temporal quadrants, (f)–(i) : NRR area obtained in Superior, Inferior, Nasal and Temporal quadrants

TABLE II. PERFORMANCE COMPARISON OF GLAUCOMA DETECTION METHODS

Method	Dataset	Sensitivity (%)	Specificity (%)	Accuracy (%)
Nayak et al. [21]	Local hospital	100	80	93.33
Burana-Anusorn et al. [22]	Local hospital	80	93	89
Narasimhan and Vijayarekha [1]	Local hospital	90.45	93.2	95
de la Fuente-Arriaga et al. [23]	Centre for Computing Research of IPN database	93.02	91.66	91.34
Khan et al. [24]	DMED, FAU, Messidor	-	-	94
Proposed Method	**HRF, Messidor, DRIONS-DB, RIM-ONE, Local hospital**	**91.82**	**95.60**	**94.14**

TABLE III. COMPARISON OF THE PROPOSED METHOD WITH OTHER TECHNIQUES IMPLEMENTED ON THE SAME DATASETS

Method	Dataset	Sensitivity (%)	Specificity (%)	Accuracy (%)
Nayak et al. [21]	HRF, Messidor, DRIONS-DB RIM-ONE, Local hospital	96.30	81.56	91.68
Khan et al. [24]	HRF, Messidor, DRIONS-DB	90.67	93.33	92
Burana-Anusorn et al. [22]	HRF, Messidor, DRIONS-DB RIM-ONE, Local hospital	88.12	92.16	90
Proposed Method	**HRF, Messidor, DRIONS-DB, RIM-ONE, Local hospital**	**91.82**	**95.60**	**94.14**

V. CONCLUSION

In this paper, we proposed a method for the detection of glaucoma based on the ISNT rule. The method uses watershed transformation for OD and OC segmentation. Circular approximation is used to approximate the segmented OD and OC. The ISNT rule is evaluated by finding the NRR areas in the ISNT quadrants. The developed method is tested on four publicly available databases, HRF, Messidor, DRIONS-DB, RIM-ONE and a local hospital database. The proposed method is simple, computationally efficient and can be used as a supportive tool in the computer-assisted screening of glaucoma. The method can be further improved by implementing an OD localization algorithm which would make it fully automatic.

REFERENCES

[1] K. Narasimhan and K. Vijayarekha, "An efficient automated system for glaucoma detection using fundus image," *Journal of Theoretical and Applied Information Technology*, vol. 33, no. 1, pp. 104–110, 2011.

[2] (2004, Nov.) Glaucoma is second leading cause of blindness globally. Bulletin of the World Health Organization. [Online]. Available: http://www.who.int/bulletin/volumes/82/11/feature1104/en/

[3] S. Bhartiya, R. Gadia, H. S. Sethi, and A. Panda, "Clinical evaluation of optic nerve head in glaucoma," *Journal of Current Glaucoma Practice*, vol. 4, no. 3, pp. 115–132, 2010.

[4] A. Jackson, "Understanding and Living with Glaucoma," pp. 1–5, 2014, http://www.glaucoma.org/. Accessed 16 October 2014.

[5] R. R. Bourne, "The optic nerve head in glaucoma," *Community Eye Health*, vol. 19, no. 59, p. 44, 2006.

[6] N. Harizman, C. Oliveira, A. Chiang, C. Tello, M. Marmor, R. Ritch, and J. M. Liebmann, "The isnt rule and differentiation of normal from glaucomatous eyes," *Archives of ophthalmology*, vol. 124, no. 11, pp. 1579–1583, 2006.

[7] A. Aquino, M. E. Gegúndez-Arias, and D. Marín, "Detecting the optic disc boundary in digital fundus images using morphological, edge detection, and feature extraction techniques," *IEEE Transactions on Medical Imaging*, vol. 29, no. 11, pp. 1860–1869, November 2010.

[8] S. Morales, V. Naranjo, D. Pérez, A. Navea, and M. Alcañiz, "Automatic detection of optic disc based on pca and stochastic watershed," in *European Signal Processing Conference*, vol. 20, August 2012, pp. 2605–2609.

[9] S. Morales, V. Naranjo, J. Angulo, and M. Alcañiz, "Automatic detection of optic disc based on pca and mathematical morphology," *IEEE Transactions on Medical Imaging*, vol. 32, no. 4, pp. 786–796, 2013.

[10] L. G. Priyadharshini M and J. Anitha, "A region growing method of optic disc segmentation in retinal images," in *2014 International Conference on Electronics and Communication Systems (ICECS)*, Feb 2014, pp. 1–5.

[11] M. V. Wyawahare and P. M. Patil, "Extraction of optic cup in retinal fundus images: A compartitive approach," *International Journal of Signal Processing, Image Processing and Pattern Recognition*, vol. 7, no. 2, pp. 389–398, 2014.

[12] R. Ingle and P. Mishra, "Cup segmentation by gradient method for the assessment of glaucoma from retinal image," *International Journal of Engineering Trends and Technology (IJETT)*, vol. 4, no. 6, pp. 2540–2543, June 2013.

[13] S. Kavitha, S. Karthikeyan, and K. Duraiswamy, "Neuroretinal rim quantification in fundus images to detect glaucoma," *International Journal of Computer Science and Network Security*, vol. 10, no. 6, pp. 134–140, June 2010.

[14] D. F. Garway-Heath, S. T. Ruben, A. Viswanathan, and R. A. Hitchings, "Vertical cup/disc ratio in relation to optic disc size: its value in the assessment of the glaucoma suspect," *British Journal of Ophthalmology*, vol. 82, no. 10, pp. 1118–1124, 1998.

[15] J. B. Jonas, W. M. Budde, and P. Lang, "Neuroretinal rim width ratios in morphological glaucoma diagnosis," *British Journal of Ophthalmology*, vol. 82, no. 12, pp. 1366–1371, 1998.

[16] G. Dougherty, *Medical image processing: techniques and applications*. Tennessee, USA: Springer Science & Business Media, 2011.

[17] A. Budai and J. Odstrcilik. (2011) High-Resolution Fundus (HRF) Image Database. Friedrich-Alexander University Erlangen-Nüremberg. https://www5.cs.fau.de/research/data/fundus-images/. Accessed 5 October 2014.

[18] MESSIDOR - TECHNO-VISION Project. (2014, March) Methods to evaluate segmentation and indexing techniques in the field of retinal ophthalmology. http://messidor.crihan.fr/. Accessed 5 October 2014.

[19] J. G. Feijoo, J. M. M. de la Casa, H. M. Servet, M. R. Zamorano, M. B. Mayoral, and E. J. C. Suárez. (2009, August) DRIONS-DB: Digital Retinal Images for Optic Nerve Segmentation Database. http://www.ia.uned.es/∼ejcarmona/DRIONS-DB.html. Accessed 10 October 2014.

[20] T. Kauppi, V. Kalesnykiene, J. K. Kamarainen, L. Lensu, I. Sorri, A. Raninen, R. Voutilainen, J. Pietilä, H. Kälviäinen, and H. Uusitalo. (2007) DIARETDB1 - Standard Diabetic Retinopathy Database Calibration level 1. Lappeenranta University of Technology. http://www.it.lut.fi/project/imageret/diaretdb1/. Accessed 16 October 2014.

[21] J. Nayak, R. Acharya U., P. Bhat, N. Shetty, and T. Lim, "Automated diagnosis of glaucoma using digital fundus images," *Journal of Medical Systems*, vol. 33, no. 5, pp. 337–346, 2009.

[22] C. Burana-Anusorn, W. Kongprawechnon, T. Kondo, S. Sintuwong, and K. Tungpimolrut, "Image processing techniques for glaucoma detection using the cup-to-disc ratio," *Thammasat International Journal of Science and Technology*, vol. 18, no. 1, p. 22, 2013.

[23] J. de la Fuente-Arriaga, E. M. Felipe-Riverón, and E. Garduño-Calderón, "Application of vascular bundle displacement in the optic disc for glaucoma detection using fundus images," *Computers in Biology and Medicine*, vol. 47, pp. 27–35, 2014.

[24] F. Khan, S. A. Khan, U. U. Yasin, I. Ul Haq, and U. Qamar, "Detection of glaucoma using retinal fundus images," in *Biomedical Engineering International Conference (BMEiCON)*, vol. 6. IEEE, 2013, pp. 1–5.